Modelling of proton transfer reactions in a bulk solution of acetonitrile molecules using path integral method

Lu Yang

2020

WESTERN UNIVERSITY

Faculty of Science

Department of Chemistry

CHEM4491E

Supervisor: Dr. Styliani Constas

Contents

Abstract

Proton transfer reactions are an important class of fundamental chemical reactions. Solvent fluctuations determine the mechanism of proton transfer reactions. In this thesis, we conduct path integral molecular dynamics simulation of a proton transfer between two negative symmetric binding sites (ions) in a bulk solution of acetonitrile (CH_3CN) molecules in order to determine the proton transfer mechanism and rate. The proton is represented by a polymer ring. The distance between the two negative ions is fixed at 7 Å. The proton migrates between these two ions. Using as a reaction coordinate the distance of the centroid of the polymer ring from the binding sites it is found that the proton mainly appears at a distance of 2.575 Å and 4.475 Å measured from one of the ions. The average free energy barrier along the centroid distance reaction coordinate is found to be 3.31+/- 0.25 kcal/mol. The natural frequency at the free energy minima is estimated to be 219.8 ps^{-1} +/- 0.25 ps^{-1}. Thus, the magnitude of proton transfer rate in the transition-state theory approximation is estimated to be 0.44 ps^{-1}. According to the previous studies, proton transfer rate is 0.2 ps^{-1} for the quantum proton bonded to a pair of A^- ions in a cluster of 40 diatomic molecules. The literature value is smaller than the experimental value of 0.44 ps^{-1} for the quantum proton bonded to a pair of A^- ions in a bulk solution of acetonitrile molecules.

Acknowledgements

I would like to thank Dr. Constas for her incredible support and guidance throughout this thesis project. With her guidance, I have become a better student, researcher, and professional. Additionally, I would like to thank the Victor Kwan for his help with the computer science aspect of this project. With his help, I got better understanding of my project and using LAMMPS and i-PI to do simulation. Lastly, I would like to thank the entire Constas group for their many useful discussions to do simulation.

List of Abbreviations

TST – transition-state theory

PI – path integral

LJ – Lenard-Jones

PIMD – Path Integral Molecular Dynamics

VMD – Visual Molecule Dynamics

MM – Molecular Mechancis

PBC – Periodic boundary conditions

MD – Molecular dynamics

RC – Reaction Coordinate

ps – Picosecond

fs – Femtosecond

1. Introduction

Proton transfer reactions are an important class of fundamental chemical reactions. In these reactions, a proton (H^+) is transferred from one species (acid) to another species (base) as shown in the following general reaction

$$AH + B^- \rightleftharpoons A^- + BH \quad (1)$$

where AH, BH are acids, B^- and A^- are bases. Reaction (1) may take place in solution, in the gaseous state or in solid state such as in ice. In this thesis we study reaction (1) in solution. Proton transfer reactions are ubiquitous in chemistry, biochemistry, electrochemistry, transmission of signals in biological systems and enzymatic reactions. A typical example in chemistry are acid-base reactions and in biochemistry are proton coupled electron transfer reactions in ribonucleotide reductase (RNR)[1]. Because of their universality proton transfer reactions have attracted a lot of attention in relevant fields. Proton has a high degree of quantum mechanical character due to its low mass, where quantum mechanical zero-point energy and tunneling effects are not negligible[2].

In recent years, a better understanding of the mechanism of proton transfer reactions in polar solvent has developed[3]-[12]. It is important to emphasize that the reaction pathway for proton transfer is determined by the solvent fluctuations due to the strong Coulombic coupling of the charge transfer in the reacting pair to the polar solvent[13]. As the orientation of solvent molecules changes due to fluctuations[14]-[17], the geometry of acid-base H-bond is affected by the macroscopic electric field generated by dipole moments of solvent molecules[18]. A schematic picture of solvent polarization influencing proton transfer reactions is shown in Fig. 1, where green

spheres are the proton binding sites, for instance these sites may be $-COO^-$ groups, orange sphere is the proton and blue arrows are the dipole moments of solvent molecules.

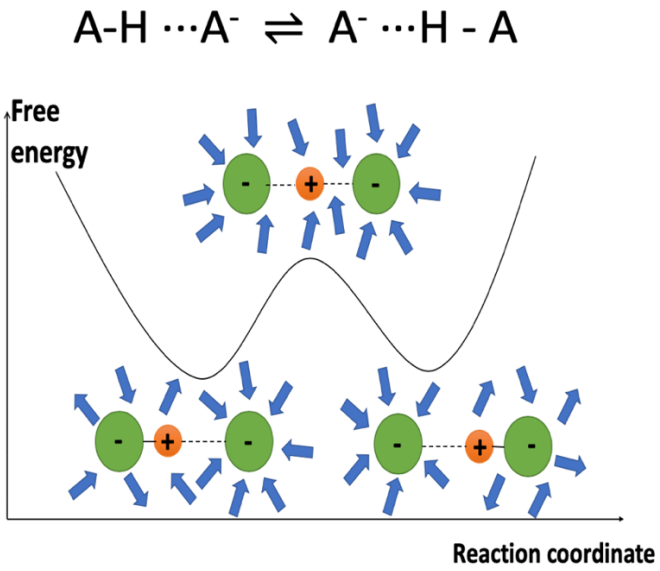

Fig 1. A schematic picture of solvent polarization influencing proton transfer reaction between two symmetric binding sites, which are ionic. The proton transfer process is quantified by the free energy profile (solid line) along a reaction coordinate. The blue arrows represent the solvent molecule dipole moment. The green spheres represent the two sites between which the proton in transferred. The two sites are identical. The orange sphere represents the proton.

Classical mechanics is unsuitable to study the rate of proton transfer reactions because proton transfer does not follow Newton's law of motion. Full quantum mechanical modelling of the protonation reaction in solvent is inefficient because of the many degrees of freedom involved, that of the proton and that of the solvent. The solvent has a huge number of degrees of freedom and the computational cost increases exponentially with the number of degrees of freedom[16]. An efficient way to study the mechanism of proton transfer reactions in polar solvent is to treat the

solvent molecules by classical mechanics and treat the proton as the diffuse proton cloud[19]. Feynman's concept of path integrals[20] provides a computationally feasible method by mapping the quantum proton partition function to that of a classical ring polymer. The polymer ring is composed of beads that are connected by harmonic springs[20]. The centroid (center of mass) of this ``classical'' proton ring polymer is often used in the calculations. The problem of proton transfer includes the analysis of the reaction mechanism and the computation of the rate constant. Calculation of a rate constant for any reaction in the condensed phase is a non-trivial task[14]. First of all the system is too complex to allow for analytical solutions and the computations of the rates often goes beyond the direct application of molecular dynamics runs.

The efficient way to study the reaction is to calculate the free energy profile along a reaction coordinate (RC) by using molecular dynamics or Monte Carlo to sample the conformational space[21]. In this study the reaction coordinate of the proton transfer reaction is the distance of the centroid of the proton polymer ring to each of the negatively charged binding sites (ions). According to the transition state theory (TST), a free energy surface connects the reactant and product states. The reactants and products correspond to minima in this free energy surface and the transition state to a saddle point. For one-dimensional reaction coordinate as the one used here, the transition state is at the maximum of the free energy profile. The proton transfer transition state theory (TST) rate (k_{TST}) can be directly computed from

$$k_{TST} = \frac{\omega_0}{2\pi} e^{\frac{-W(\xi^+)}{k_B T}} \qquad (2)$$

where ω_0 is the frequency at the free energy minimum and W is the free energy difference between the maximum of the profile (transition state) and one of the minimum (reactant or product state in the symmetric case we study), ξ^+ is the location (units of length) of the transition state. k_B

is the Boltzmann's constant and T is the temperature and held constant using the Langevin thermal bath.

This work will focus on the study of proton transfer in a bulk solution. The bulk solution is modelled by using periodic boundary conditions to avoid the effect of the boundaries. This work will use path integral molecular dynamics (PIMD) to study a model proton transfer reaction between two symmetric sites. Details will be discussed in the methodology section. Several methods can calculate the free energy barrier along the RC of the location of the centroid[22]-[25].

The structure of the thesis is as follows: The methodology is described in Sec 2. In Sec 3, a) analysis of the solvent polarization, b) the frequency of finding the proton at certain distance from the proton to each of the chloride ion, c) the average force potential (free energy) of proton transfer between two chloride atoms, d) proton transfer rate will be discussed. The thesis closes with the conclusion in Sec 4.

2. Methodology

2.1 Overview of Path integral Molecular Dynamics

PIMD method has been successful in the study of electronic properties of molecules at certain molecular geometries[26]. Anharmonicity, tunneling, and low-frequency "floppy" motion will lead to extremely delocalized nuclear distributions[27], which results in solving the Schrödinger equation for protons becoming a difficult task. Feynman's path integral method[20] provides a computationally feasible alternative by using the path integral (PI) formalism[20] to treat protons systems.

A fundamental equation in path integrals is Trotter's theorem, which states that given two operators $\hat{A}$ and $\hat{B}$ holds

$$e^{(\hat{A}+\hat{B})} = \lim_{n\to\infty}\left[e^{\frac{\hat{A}}{n}}e^{\frac{\hat{B}}{n}}\right]^n . \quad (3)$$

Consider the Hamiltonian ($\hat{H}$) which takes the form

$$\hat{H} = \frac{P^2}{2m} + U(X) = \hat{T} + \hat{V} \quad (4)$$

where $\hat{T}$ is the kinetic energy operator and $\hat{V}$ is the potential energy operator, which equal the potential energy U(X) of the system – X is a collective notation for all the degrees of freedom in the system. The Hamiltonian is the operator of the energy of the system. Differently, from the kinetic energy operator (which includes the Laplacian operator), the potential energy is a scalar but we still use the hat in its notation for consistency with the kinetic energy operator and Hamiltonian. It is remined here that several textbooks do not use the operator notation for the V, in order to indicate that it is a scalar. Then according to Eq (3), the Boltzmann operator using Eq (4) can be written as

$$e^{-\beta\hat{H}} = e^{-\beta(\hat{T}+\hat{V})} = \lim_{p\to\infty}\left[e^{\frac{-\beta\hat{T}}{p}}e^{\frac{-\beta\hat{V}}{p}}\right]^{\mathrm{P}} = \lim_{p\to\infty}\hat{\Omega}^{\mathrm{P}} \quad (5)$$

where P is the Trotter number and $\beta = \frac{1}{k_B T}$. $\hat{\Omega}$ equals $e^{\frac{-\beta\hat{T}}{p}}e^{\frac{-\beta\hat{V}}{p}}$. It is noticed that the time-evolution operator U(t) in the time-dependent Schrödinger equation has the same form as the quantum Boltzmann operator, with the time taking the imaginary value $t = -i\hbar\beta$. The quantum time evolution operator is written as:

$$U(t) = e^{-iHt/\hbar} \quad (6)$$

where $\hbar$ is Planck's constant and i is imaginary. This makes the space of Feynman paths doable to sample. Feynman paths can be represented efficiently using 'ring polymers', which is a set of "beads" coupled by harmonic springs as shown in Fig. 2. The Trotter number P (Eq. 5) is the number of beads in the polymer ring.

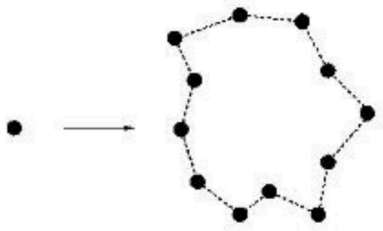

FIG 2. Ring polymer representation of a quantum particle[28]. The quantum particle shown by a black dot on the left is mapped into a polymer ring composed of beads (black dots) connected with harmonic springs.

Feynman first suggested that the path centroid (as explained later, the centroid is the center of mass of the polymer ring shown in Fig. 2) is the most classical-like variable in an equilibrium quantum system[20]. The path centroid variable is the imaginary average of a particular closed Feynman path $q(\tau)$ and is written as

$$x_c = \frac{1}{\hbar\beta}\int_0^{\hbar\beta} d\,\tau\, q(\tau)\ .\ (7)$$

In the discretized path integral picture, the path centroid variable is equivalent to the center of mass of the polymer ring, which is the geometrical average of its position over all the beads (Fig. 3).

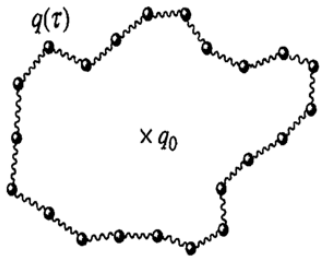

FIG 3. A discretized Feynman path $q(\tau)$ within the imaginary time interval $0 \le \tau \le \hbar\beta$.[29]

The path centroid variable of the ring polymer is given by

$$x_c = \frac{1}{p}\sum_{i=1}^{p} q_i\ .\ (8)$$

Based on the path integral formulation, for the nuclei treated as quantum particles, the canonical partition function (Z) of this system is provided by the equilibrium sampling of the set of coupled beads, written as

$$Z = tr\left[e^{-\beta\hat{H}}\right] = \int dq_1 < q_1 \vee e^{-\beta(\hat{T}+\hat{V})} \vee q_1 > \quad (9)$$

where 'tr' indicates a trace of a matrix (it is reminded that the trace of a matrix is defined as the sum of the diagonal matrix elements). According to Eq (9), the canonical partition function can be rewritten as:

$$Z = \lim_{Z\to\infty} Z_p = \lim_{Z\to\infty}\left(\frac{mp}{2\pi\beta\hbar^2}\right)^{p/2}\int dx_c e^{-\beta W(x_c)}\ .\ (10)$$

Thus, the ensemble average of an equilibrium quantity A is expressed as

$$A = \frac{1}{Z}tr\left[e^{-\beta\hat{H}}\hat{A}\right] = \frac{1}{Z}\int dq_1 < q_1 \vee e^{-\beta\hat{H}} \vee q_1 > A(q_1)\ .\ (11)$$

Therefore, the path integral method exploits the fact that the partition function of a quantum mechanical system under imaginary time is formally equivalent to the configuration integral of a classical ring polymer. As a result, the equilibrium quantum statistical properties can be obtained by using suitably classical molecular dynamics[30]. The PIMD can describe the interaction between the quantum system and the classical solvent at finite temperature[31]. PIMD is powerful because it can run as extended classical molecular dynamics simulations, generating classical trajectories. The free energy surface may be obtained by mean-field averaging the quantum Boltzmann distribution around the centroid of the ring-polymers[32].

2.2 Molecular Dynamics

Molecular dynamics (MD)[33] is a computer simulation method for analyzing the physical movements of atoms and molecules. MD generates the trajectory of a giving system by solving Newton's equation of motion for each atom and molecule by discretizing the positions of the atoms using a small time step. Newton's 2nd law that underlies MD[33] is written as

$$\vec{F} = m\vec{a} == m\frac{d^2\vec{r}}{dt^2} \quad (12)$$

where $\vec{F}$ is the sum of forces acting on a specific atom, m is the mass of a specific atom, $\vec{a}$ is the second derivative of the position with respect to time, $\vec{r}$ is the position of each atom and t is the time.

The computations handle the long-range electrostatic interactions between particles and all their infinite periodic images efficiently by Ewald summation[34]. In this method, the long-range electrostatic interactions are divided into two parts: a short-range contribution and a long-range contribution which does not have a singularity. The short-range contribution is calculated in real

space. The long-range contribution which does not have a singularity is calculated by Fourier transform[34].

2.3 Molecular Mechanics Force Fields

In molecular simulation, it is important to define all interactions between the atoms in the system being modelled, including bonding and nonbonded interactions, as well as the intermolecular and intramolecular interactions when computing the potential energy[35]. In this thesis, Molecular Mechanics (MM) force field was used to model the interactions between solvent-solvent and solvent-ion interactions. Force fields calculate the potential energy of each atom in a system by considering an average "atom'' that includes the nuclear and electronic positions merged together. The calculations of force fields are done by summing the stretching, angle bending, torsion interactions and non-bonded interactions. The equation for calculation of force fields is the following[35]:

$$U(\bar{r}^N) = \sum_{bonds} \frac{K_b}{2}(l_i - l_0)^2 + \sum_{angles} \frac{K_\theta}{2}(\theta_i - \theta_0)^2 + \sum_{torsions} \frac{V_n}{2}(1 + cos(n\omega - \gamma)) +$$

$$\sum_i^{N-1} \sum_{j=i+1}^{N} (4 \in_{ij} [(\frac{\sigma_{ij}}{r_{ij}})^{12} - (\frac{\sigma_{ij}}{r_{ij}})^{6}] + \sum_{j=i+1}^{N} \frac{q_i q_j}{4\pi\epsilon_0 r_{ij}}) \quad (13)$$

where $U(\bar{r}^N)$ is the potential energy of the system as a function of the positions r of all N atoms. U is a function of all the coordinates of the atoms in the system (thus, 3N coordinates for the N atoms) and we collectively show these coordinates by $\bar{r}^N$. K_b is a force constant of the harmonic spring and K_θ is the force constant that corresponds to the angle of vibration. l_i and l_0 are the deviated position and equilibrium bond length of the harmonic spring, respectively. θ_i and θ_0 are the deviated and equilibrium bond angles of the bending of adjacent bonds. V_n is the torsion barrier. γ is the torsion equilibrium value. ω is the angle deviation from the equilibrium angle γ. The potential terms for non-bonded interactions are described in a pair-wise manner with LJ and

Coulomb terms. $4 \in_{ij} (\frac{\sigma_{ij}}{r_{ij}})^{12}$ represents repulsive forces between two atoms due to the Pauli Exclusion Principle. $-4 \in_{ij} (\frac{\sigma_{ij}}{r_{ij}})^{6}$ represents attractive interaction arising from the London dispersion forces. The final term $\frac{q_i q_j}{4\pi\epsilon_0 r_{ij}}$ expresses Coulomb's Law, where q_i and q_j are the partial charges for two atomic sites. ϵ_0 is the permittivity of the vacuum, and r_{ij} is the distance between two atomic sites i and j.

2.4 Model system and simulation method

2.3.1 Computational parameters

The system consists of a proton and two chloride ions in a bulk solution where the central simulation box has 40 acetonitrile molecules (CH_3CN). The central box is cubic and it is replicated by using periodic boundary conditions (PBC). Acetonitrile has been selected as a solvent because it is aprotic, i.e. its hydrogen atoms do not participate in proton transfer reactions. The use of an aprotic solvent allows us to focus on a specific proton transfer process, instead of many proton transfer reactions that may happen simultaneously in as in a water solvent for example. The proton is transferred between two symmetric negatively charged sites. The two negative sites are modelled by chloride ions, but the model of ions is general and one can use any other ions. During MD, the distance between the two chloride ions is fixed at 7 Å. The proton migrates between those two chloride ions.

The simulation was performed in a box of about $22.49 \times 22.43 \times 12.24$ Å with PBC[36]. A schematic picture of periodic boundary conditions is shown in Fig 4. PBC can remove the surface interactions of the molecules on the surface of the simulation box. Based on Fig 4, the

cubic box is replicated through space to form an infinite lattice. Therefore, when a particle moves in the original box, the particle moves in each of the neighboring boxes in exactly the same way[36].

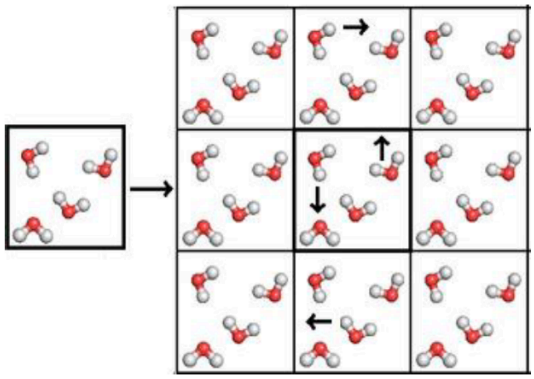

Fig 4. A schematic picture of periodic boundary conditions.

Each simulation was run in the canonical ensemble (NVT – where N is the number of molecules in the system, V – the volume of the system and T- the temperature of the system) to stabilize the temperature. The temperature was initialized at 200 K and held constant using the Langevin thermal bath[37] with a time constant of 5 fs. A snapshot of the simulated model system of 40 acetonitrile molecules is shown in Fig 5 (a), where the yellow sphere is the proton and two green spheres are the chloride ions.

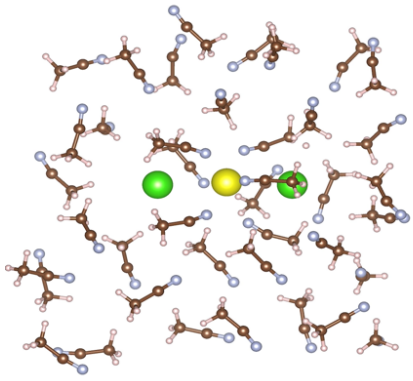

FIG 5. A snapshot of the simulated model system of a proton and two chloride ions in bulk solutions of 40 acetonitrile molecules (CH_3CN) with PBC. The chloride and proton ions have been enlarged for visualization purpose.

CGENFF force field was used. The number of beads in the polymer ring is 12. Increasing the number of beads does not change the result. Each simulation was run for 200 ps with a timestep of 0.25 fs. Parameters of mass, charge and LJ potential energy for the acetonitrile molecules, two chloride ions and proton are shown in Table. 1.

	Atom types	Mass (amu)	charge	LJ potential (J)
HGA3	$C'H_3'CN$	1.008	+0.09	0.024
CG1N1	$'C'H_3CN$	12.011	+0.36	0.18
CG331	$CH_3'C'N$	12.011	- 0.17	0.01
NG1T1	$CH_3C'N'$	14.007	- 0.46	0.18
CLA	Chloride ions	35.45	-1	0.15
SOD	Proton	1.008	+1	0.0469

Table 1. Parameters (mass, charge, LJ potential) of the acetonitrile, the model ions and the model proton.

All simulations in this thesis were performed using the i-PI[38] and LAMMPS[39]. i-PI is a Path Integral Molecular Dynamics (PIMD). The implementation is based on a client-server paradigm, where i-PI acts as the server and LAMMPS as the client. i-PI deals with the propagation of the nuclear dynamics and runs the PIMD calculation. LAMMPS deals with the calculation of the

forces, potential energy and kinetic energy. Visualization of all trajectories and subsequent analysis were done using Visual Molecular Dynamics (VMD) version 1.9.4[40].

2.3.2 Method of Analysis

The main objective of this work is the calculation of the rate of proton transfer at the transition state theory approximation. In order to calculate the rate of proton transfer rate, a reaction coordinate of the distance of the proton polymer ring centroid from each of the ions is used. The potential of mean force (free energy) can be calculated as follows[41]:

$$g(r) = e^{-\frac{W}{k_B T}}$$

$$W = -\ln\left[g(r)\right]kT \quad (14)$$

where g(r) is radial distribution function, W is the potential of mean force**,** k_B is the Boltzmann constant and T is the temperature. In order to obtain the value of the frequency at the free energy minima, a quadratic function was fitted to the minimum. The value of natural frequency can be calculated as follows[42]:

$$r(x) = \mathrm{a} \cdot \cos(\omega t + \varphi) \quad (15)$$

where r(x) is the distance for the proton to each of the ions, a is the amplitude of the oscillator, ω is the angular frequency of the simple harmonic motion, t is the time, φ is the phase constant and determined by the initial conditions of the motion. The transition state rate constant for the proton transfer can be calculated[43] by

$$k_{TST} = \frac{\omega_0}{2\pi} e^{\frac{-W(\xi^+)}{k_B T}} \quad (2)$$

where the variables have the same meaning as in Eq (2).

3 Results and Discussion

3.1 Analysis of the solvent polarization

Typical snapshots of the proton transfer reaction in a bulk solution of 40 acetonitrile molecules with PBC is shown in Fig 6. Figure 6 (a) shows the initial state of proton transfer reactions in a bulk solution of 40 acetonitrile molecules with PBC. The distance between proton to the left-side chloride ion is 2.575 Å which calculated by VMD. Fig 6 (b) shows the transition state of proton location. The distance between proton to the left-side chloride ion is 3.525 Å which calculated by VMD. Figure 6 (c) shows the transferred proton. The distance between proton to the left-side chloride ion is 4.475 Å which calculated by VMD. Figure 6 clearly shows that the proton transfers from left-side chloride ion to right-side chloride ion in the bulk solution. Besides, the black sphere is the nitrogen atom of acetonitrile molecule. The direction of dipole moment is $CH_3 - \overrightarrow{C \equiv N}$.

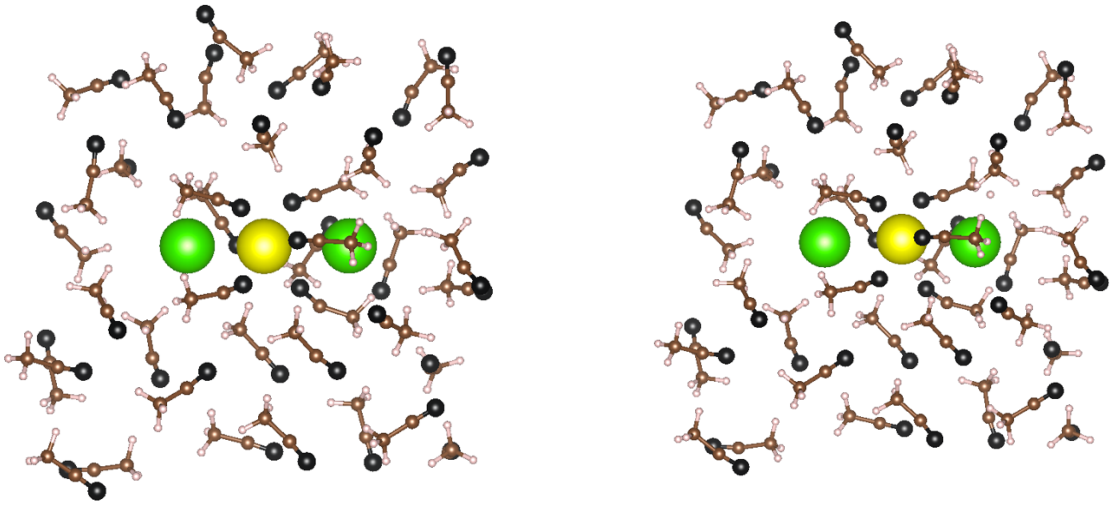

(a) (b)

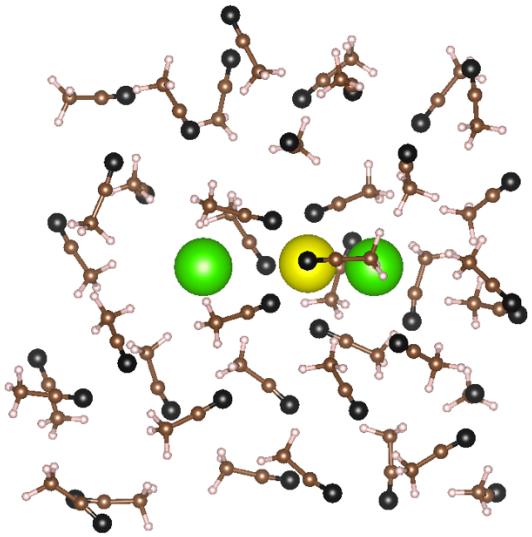

(c)

FIG 6. Snapshots of the proton transfer reactions in a bulk solution of 40 acetonitrile molecules. (a) shows the initial state of proton where located close to the left-side chloride ion, and the dipole moment of acetonitrile molecules point to the right-side chloride ion, (b) shows the transition where the solvent molecules tend to aggregate around the proton-ion complex symmetrically and (c) shows the transferred proton where located close to the right-side chloride ion, and the dipole moment of acetonitrile molecules point to the left-side chloride ion.

The proton transfer reaction is influenced by the fluctuations of the solvent molecules in a bulk solution of 40 acetonitrile molecules due to the strong Coulombic coupling of the charge transfer in the reaction pair to the polar solvent. Therefore, solvent polarization plays an important role in determine the character of the proton transfer reaction. Without solvent molecules, proton transfer reactions will not happen. In the product or reactants states, the complex $(A-H\cdots A^{-})$ or $(A^{-}\cdots H-A)$ have the structure of the proton more tightly bound one side of chloride ion and more distant to another side of chloride ion. In this case, the solvent molecules tend to strongly

solvate the part of the proton-ion complex with the more exposed negative charge, which means the $\cdots A^-$ part experiences strong charge-dipole interactions with the solvent molecules. The dipole moment of $A-H$ dipole is smaller than the solvent molecules. Therefore, the interaction between $A-H$ end of the proton-ion complex and solvent dipolar molecules is much weaker than the solvent-solvent interaction. The orientation of solvent molecules changing results in the polymer chain to fluctuate more freely, the geometry of acid-base H-bond is affected by the electric field generated by dipole moment of solvent molecules, which results in proton transfer reactions happening. In the transition state, the solvent molecules tend to aggregate around the proton-ion complex symmetrically, and the dipole moment of positive ions towards the proton-ion complex, which results in inhibiting the fluctuations of the polymer chain[35].

3.2 Computation of free energy and TST rate

Initially, a histogram of the values of the RC is obtained by counting the values of the RC in bins. The bin size is 0.05. The frequency of finding the proton at certain distance from the proton to each of the chloride ion was obtained by collecting the values of the RC in a long, unconstrained MD run. The references ions, which are the two chloride ions, are located at r=0 Å and r=7 Å. A histogram of the values of RC normalized by the volume element is shown in Fig. 7. Figure 7 shows the probability distribution of the proton moving between the two chloride ions. The maxima of the distribution indicate that the proton mainly appears at 2.575 Å and 4.475 Å, respectively.

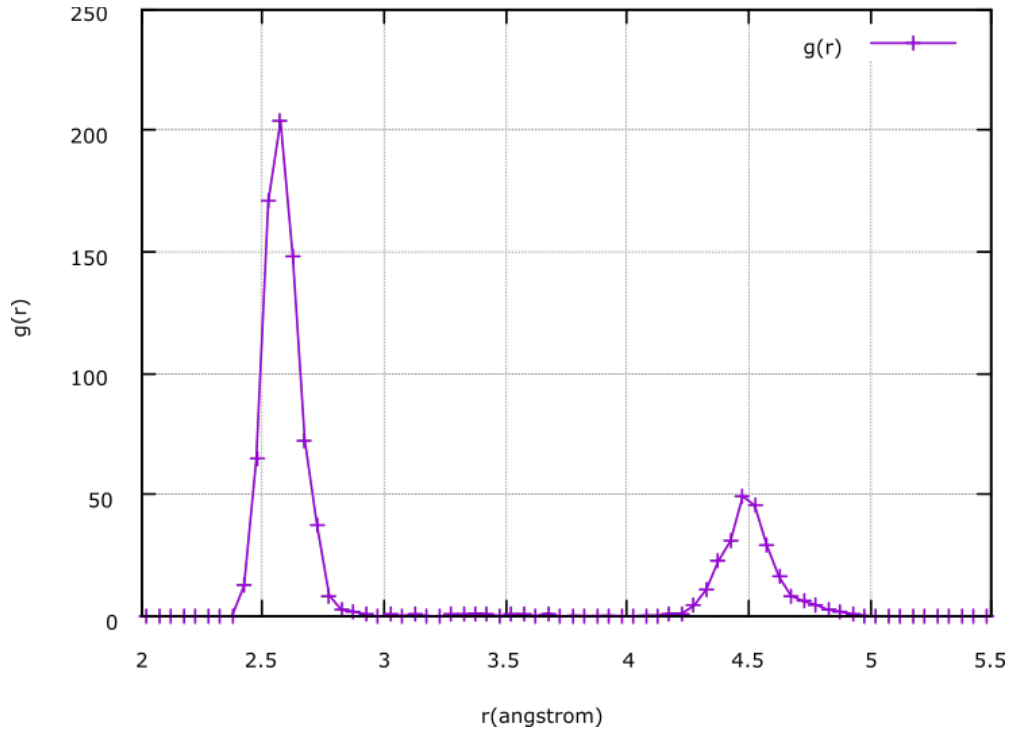

Fig 7. The relationship between distance and the probability distribution of the proton.

After obtaining the frequency of finding the proton at distance r, the average force potential (free energy) can be obtained directly from Eq (14)[33]. By those calculations, the free energy as a function of the reaction coordinate associated with moving the proton along the reaction path can be obtained as shown in Fig. 8. According to Fig 8, the minimum energies and maximum energies of the proton transfer reaction are not equal. The two binding sites (chloride ions) are symmetric. Thus, one would expect that the two maxima in Fig. 7 should have the same height. The difference in height is attributed to poor statistics. The simulation run is not long enough to allow for the acetonitrile molecules to diffuse sufficiently and rotate. Since the proton mainly appears at 2.575 Å and 4.475 Å, the lowest energies can be found at 2.575 Å and 4.475 Å, based on the Eq (14), which are -3.11+/- 0.25 and -2.26+/- 0.25 kcal/mol. Two highest energies also can be found at 3.175 Å and 3.975 Å based on the Eq (12), which are 0.45 +/- 0.25 and 0.80 +/- 0.25 kcal/mol

respectively. After obtaining the two lowest energies and the two highest energy, the two energy barriers can be calculated as the difference in free energy between the top and the minimum, which are 3.56+/- 0.25 kcal/mol and 3.06+/- 0.25 kcal/mol. Therefore, the average free energy barrier along the centroid distance reaction coordinate is found to be 3.31+/- 0.25 kcal/mol.

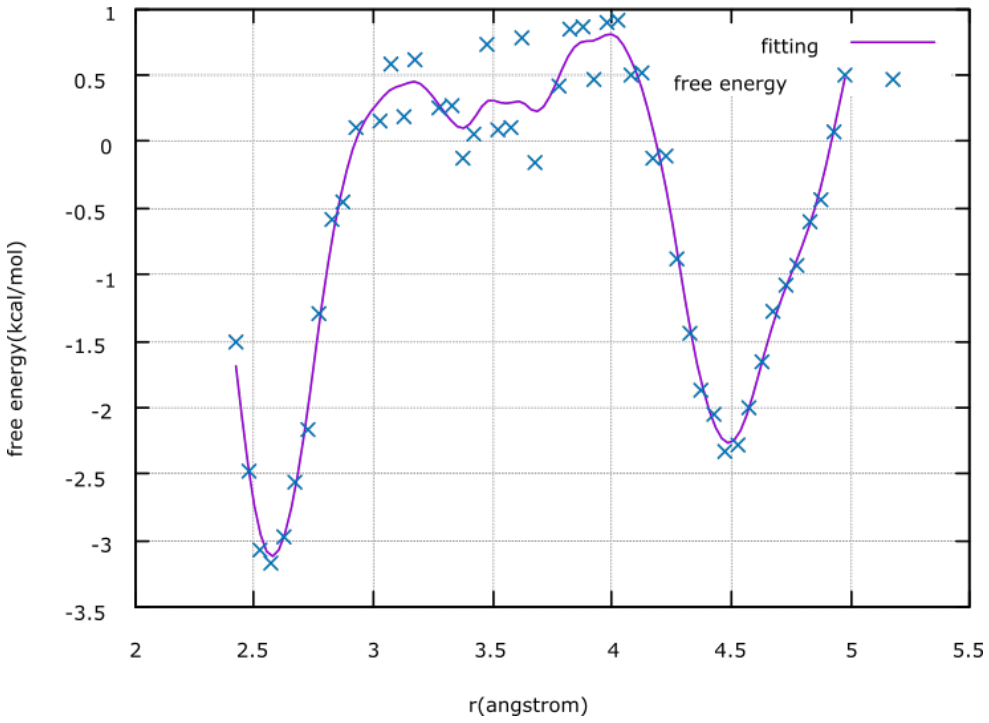

Fig 8. Free energy profile along the centroid reaction coordinate in the ring polymer representation of the proton

The transition state theory shown in Eq. (2) is used for the calculation of the proton transfer rate. In order to obtain the value of the frequency at the free energy minima, the function shown in Fig. 8 is fitted by a quadratic function at its minima. The value of natural frequency can be obtained directly from Eq (15). A histogram representing (Fig 9 and Fig 10) can be obtained with the relationship between the time and the distance of the proton to each side of chloride ions. Figure

9 shows the relationship between time and the distance of the proton to the left-side chloride ion. The equation is $r(x) = 0.082545 \cdot \cos(219.557x - 47.6241) + 2.58002$. Based on the equation, $\omega_L = 219.56 +/- 0.25$ ps^{-1}.

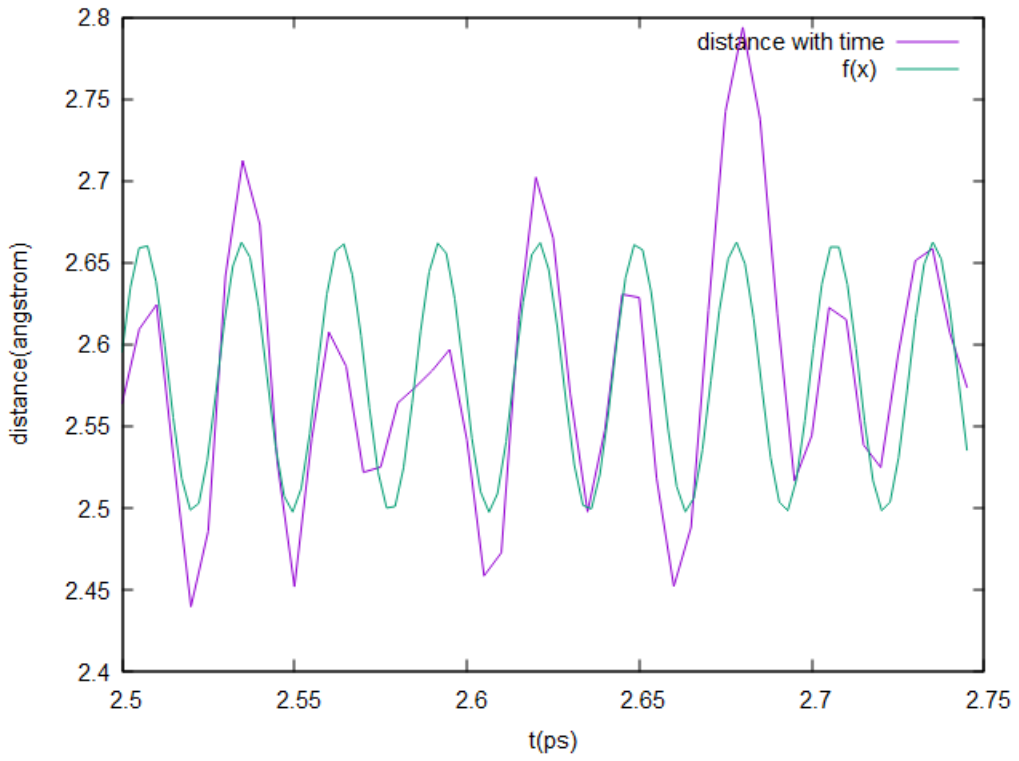

Fig 9. The relationship between the time and the distance of the proton to the left-side chloride ion.

Figure 10 shows the relationship between time and distance of the proton to the right-side chloride ion. The equation is $r(x) = 0.0788545 \cdot \cos(220.051x - 52.0659) + 4.44699$. Based on the equation, $\omega_R = 220.051 +/- 0.25$ ps^{-1}.

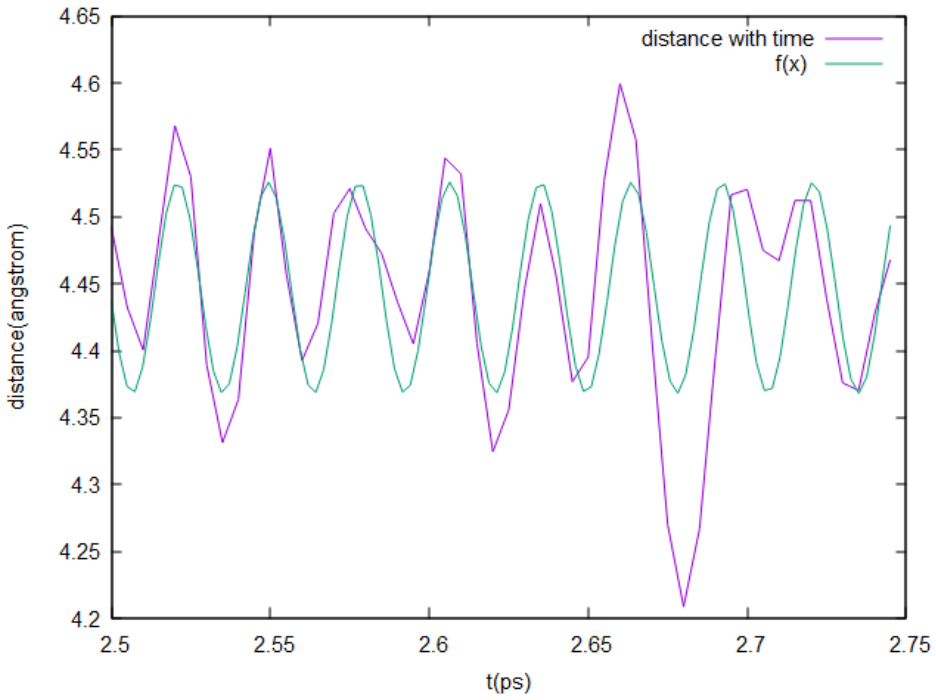

Fig 10. The relationship between the time and the distance of the proton to the right-side chloride ion.

As above, the natural frequencies are 219.56+/- 0.25 ps^{-1} and 220.051+/- 0.25 ps^{-1} from each side of chlorine atoms respectively. The average frequency at the free energy minima is estimated to be 219.8+/- 0.25 ps^{-1}. The proton transfer rate can be calculated directly from Eq (2): The proton transfer rate for the proton to the left-side and right-side chloride ions can be calculated directly from Eq (2):

$$k_{left} = \frac{\omega_0}{2\pi} e^{\frac{-W(\xi^+)}{KT}} = \frac{219.56\, ps^{-1}}{2\pi} e^{\frac{-5.317KT}{KT}} = 0.171\, ps^{-1}$$

$$k_{right} = \frac{\omega_0}{2\pi} e^{\frac{-W(\xi^+)}{KT}} = \frac{220.051\, ps^{-1}}{2\pi} e^{\frac{-3.901\, KT}{KT}} = 0.708\, ps^{-1}$$

Therefore, the proton transfer rates are 0.171 ps^{-1} and 0.708 ps^{-1}. The average proton transfer rate is 0.44 ps^{-1}. The large differences in the values between the two proton transfer rates is due to poor

statistics. According to the previous studies, proton transfer rate is 0.2 ps^{-1} for the quantum proton bonded to a pair of A^- ions in a cluster of 40 diatomic molecules[14]. The literature value is smaller than the experimental value of 0.44 ps^{-1} for the quantum proton bonded to a pair of A^- ions in a bulk solution of acetonitrile molecules with periodic boundary conditions.

Based on the result, it clearly shows that proton transfer reactions are fast. The reason for the fast proton transfer is that proton can tunnel through barriers without go over the barrier in an activated process due to the low mass of the proton. Proton tunneling becomes particularly important at low temperature because the available thermal energy at low temperature may be inadequate for an activated process to occur. Besides, proton transfer rates for the proton transferring to the left-side chloride ion and to the right-side chloride ion are different most likely due to limited length of the simulation run. The rate calculation is based on the TST estimate, thus the next step of the calculation is to compute the transmission coefficient, which are the re-crossing corrections at the barrier top. The transmission coefficient is a correction over the TST theory and has not been performed in this study.

4 Conclusion

In this thesis, path integral molecular dynamics investigation on a proton transfer between two chloride ions in a bulk solution of acetonitrile molecules (CH_3CN) was conducted to determine the proton transfer rate. During the dynamics process, the two chloride ions are fixed at distance of 7 Å. The proton migrates between those two chloride ions.

The reaction pathway for proton transfer is determined by the solvent fluctuations due to the strong Coulombic coupling of the charge transfer in the reacting pair to the polar solvent. As the orientation of solvent molecules changes due to fluctuations, the geometry of chloride ion – proton bond is affected by electric field generated by dipole moments of solvent molecules. Firstly, it was found that the proton mainly appears at 2.575 Å and 4.475 Å distance form each chloride atom, respectively, which corresponds to the free energy minima along the distance reaction coordinate. Secondly, the two lowest energies are -3.11+/- 0.25 and -2.26+/- 0.25 kcal/mol respectively and the highest energies are 0.45+/- 0.25 and 0.80+/- 0.25 kcal/mol. The average barrier height is the difference between the minimum and the barrier top, which is 3.31+/- 0.25 kcal/mol. Further, transition state theory is used to calculate the proton transfer rate. By fitting the free energy data to a harmonic oscillator, the natural frequency at the free energy minima are estimated to be 219.56+/- 0.25 and 220.051+/- 0.25 ps^{-1}, respectively. The average natural frequency at the free energy minima is 219.8+/- 0.25 ps^{-1}. Application of the transition state theory yields the average proton transfer rate as 0.44 ps^{-1}. According to the previous studies, proton transfer rate is 0.2 ps^{-1} for the quantum proton bonded to a pair of A^- ions in a cluster of 40 diatomic molecules. The literature value is smaller than the experimental value of 0.44 ps^{-1} for the quantum proton bonded to a pair of A^- ions in a bulk solution of acetonitrile molecules with periodic boundary conditions. The reason for the proton transfer is fast is that a proton can tunnel through barriers without go over the barrier in an activated process due to the low mass of the proton. Since the two negative sites are identical any asymmetries in the free energy profile and rate are due to statistical reasons. The next step in the analysis is to correct the transition state theory estimate of the rate by estimating the transmission coefficient. This will allow the computation of the full rate constant of the proton transfer reaction.

References

[1] M. R. A. Blomberg, P. E. M. Siegbahn, *Biochim. Biophys. Acta - Bioenerg.* **2006**, *1757*, 969–980.

[2] A. Douhal, F. Lahmani, A. H. Zewail, *Chem. Phys.* **1996**, DOI 10.1016/0301-0104(96)00067-5.

[3] W. Xie, Y. Xu, L. Zhu, Q. Shi, *J. Chem. Phys.* **2014**, *140*, DOI 10.1063/1.4873135.

[4] T. Yamamoto, W. H. Miller, *J. Chem. Phys.* **2005**, *122*, DOI 10.1063/1.1832598.

[5] R. Collepardo-Guevara, I. R. Craig, D. E. Manolopoulos, *J. Chem. Phys.* **2008**, *128*, DOI 10.1063/1.2883593.

[6] S. Daschakraborty, P. M. Kiefer, Y. Miller, Y. Motro, D. Pines, E. Pines, J. T. Hynes, *J. Phys. Chem. B* **2016**, *120*, 2281–2290.

[7] J. P. Bothma, J. B. Gilmore, R. H. McKenzie, *New J. Phys.* **2010**, *12*, DOI 10.1088/1367-2630/12/5/055002.

[8] P. M. Kiefer, J. T. Hynes, *J. Phys. Org. Chem.* **2010**, *23*, 632–646.

[9] R. P. McRae, G. K. Schenter, B. C. Garrett, Z. Svetlicic, D. G. Truhlar, *J. Chem. Phys.* **2001**, *115*, 8460–8480.

[10] Q. Zhang, G. Wahnström, M. E. Björketun, S. Gao, E. Wang, *Phys. Rev. Lett.* **2008**, DOI 10.1103/PhysRevLett.101.215902.

[11] R. L. Hayes, S. J. Paddison, M. E. Tuckerman, *J. Phys. Chem. B* **2009**, DOI 10.1021/jp907853p.

[12] M. K. Lee, P. Huo, D. F. Coker, *Annu. Rev. Phys. Chem.* **2016**, DOI 10.1146/annurev-physchem-040215-112252.

[13] S. Hammes-Schiffer, A. V. Soudackov, *J. Phys. Chem. B* **2008**, DOI 10.1021/jp805876e.

[14] S. Consta, R. Kapral, *J. Chem. Phys.* **1994**, *101*, 10908–10914.

[15] S. Consta, R. Kapral, *J. Chem. Phys.* **1996**, DOI 10.1063/1.471153.

[16] D. Laria, G. Ciccotti, M. Ferrario, R. Kapral, *Chem. Phys.* **1994**, *180*, 181–189.

[17] M. Ferrario, D. Laria, G. Ciccotti, R. Kapral, *J. Mol. Liq.* **1994**, *61*, 37–47.

[18] I. G. Shenderovich, G. S. Denisov, *Molecules* **2020**, *25*, 436.

[19] A. Staib, D. Borgis, J. T. Hynes, *J. Chem. Phys.* **1995**, DOI 10.1063/1.468678.

[20] R. P. (Richard P. Feynman, A. R. Hibbs, *Quantum Mechanics and Path Integrals*, McGraw-Hill, **1965**.

[21] J. Mavri, H. J. C. Berendsen, W. F. Van Gunsteren, *J. Phys. Chem.* **1993**, *97*, 13469–13476.

[22] K. Ando, J. T. Hynes, *J. Phys. Chem. B* **1997**, DOI 10.1021/jp970173j.

[23] D. Li, G. A. Voth, *J. Phys. Chem.* **1991**, DOI 10.1021/j100178a033.

[24] X. Wu, W. Thiel, S. Pezeshki, H. Lin, *J. Chem. Theory Comput.* **2013**, DOI 10.1021/ct400224n.

[25] M. S. Islam, R. A. Davies, J. D. Gale, *Chem. Mater.* **2001**, DOI 10.1021/cm010005a.

[26] M. Shiga, A. Nakayama, *Chem. Phys. Lett.* **2008**, *451*, 175–181.

[27] Y. Ogata, Y. Kawashima, K. Takahashi, M. Tachikawa, *Phys. Chem. Chem. Phys.* **2015**, *17*, 25505–25515.

[28] D. Chandler, P. G. Wolynes, *J. Chem. Phys.* **1981**, *74*, 4078–4095.

[29] J. Cao, G. A. Voth, *J. Chem. Phys.* **1993**, *100*, 7.

[30] R. Quhe, M. Nava, P. Tiwary, M. Parrinello, *J. Chem. Theory Comput.* **2015**, DOI 10.1021/ct501002a.

[31] D. Marx, J. Hutter, *Ab Initio Molecular Dynamics: Basic Theory and Advanced Methods*, **2009**.

[32] G. Trenins, M. J. Willatt, S. C. Althorpe, *J. Chem. Phys.* **2019**, *151*, 054109.

[33] M. P. Allen, D. J. Tildesley, *Computer Simulation of Liquids*, Clarendon Press, **1987**.

[34] A. Y. Toukmaji, J. A. Board, *Comput. Phys. Commun.* **1996**, DOI 10.1016/0010-4655(96)00016-1.

[35] I. Pettersson, T. Liljefors, John Wiley & Sons, Ltd, **2007**, pp. 167–189.

[36] T. Zurich, T. Sciences, *Structure* **1969**.

[37] S. Attal, A. Joye, *J. Funct. Anal.* **2007**, DOI 10.1016/j.jfa.2006.09.019.

[38] V. Kapil, M. Rossi, O. Marsalek, R. Petraglia, Y. Litman, T. Spura, B. Cheng, A. Cuzzocrea, R. H. Meißner, D. M. Wilkins, et al., *Comput. Phys. Commun.* **2019**, *236*, 214–223.

[39] S. Plimpton, *Fast Parallel Algorithms for Short-Range Molecular Dynamics*, **1995**.

[40] W. Humphrey, A. Dalke, K. Schulten, *J. Mol. Graph.* **1996**, *14*, 33–38.

[41] B. G. Levine, J. E. Stone, A. Kohlmeyer, *J. Comput. Phys.* **2011**, *230*, 3556–3569.

[42] P. Musik, *Development of Computer-Based Experiment Set on Simple Harmonic Motion of Mass on Springs*, **2017**.

[43] I. H. Katzarov, A. T. Paxton, *SteelyHydrogen2014 Conf. Proc.* **2014**.

[44] M. H. V. Huynh, T. J. Meyer, *Chem. Rev.* **2007**, DOI 10.1021/cr0500030.

A Appendices

A.1 Initial input

Three input files are needed to start the simulations, which are the topology file val_solv.psf, the coordinate file val_solv.pdb, and the force field file par_all22_prot.inp. The topology file contains all the information about the structure and connectivity of atoms in the system as well as few parameters of the force field. The coordinate file contains the coordinates of the initial structure. The force field file provides virtually all the parameters for CGENFF force field, which include parameters for bond angle, length, dihedral angle, improper and Lenard-Jones potentials.

A.2 input file for LAMMPS

```
units          real

atom_style      full
bond_style      harmonic
angle_style     charmm
dihedral_style  charmm
pair_style      lj/charmm/coul/long 8 12 # CONSIDER USING VACUUM COND.
lj/charmm/coul/charmm 999 999
pair_modify     mix arithmetic
kspace_style    pppm 1e-6 # kspace_style none if lj/charmm/coul/charmm

read_data       3acn_s.data

# INSERT I-PI SETTING HERE (fix ipi ... , dump ... etc.)



#########################################################
#
# UNUSED LAMMPS SETTINGS
#
#########################################################

#special_bonds   charmm
#thermo          10
#thermo_style    multi
#timestep        1.0

#minimize 0.0 0.0 50 200

#reset_timestep  0
#fix             1 all nve
#fix             2 all shake 1e-6 500 0 m 1.0
#velocity        all create 0.0 12345678 dist uniform

#restart         500 3acn_s.restart1 3acn_s.restart2
#dump            1 all atom 100 3acn_s.dump
#dump_modify     1 image yes scale yes

#thermo          100
#run             1000
```

A.3 input file for i-PI

```
<simulation verbosity='high'>
  <output prefix='simulation'>
    <properties stride='1' filename='out'> [ step, time{picosecond}, conserved,
temperature{kelvin}, kinetic_cv, potential,kinetic_md, pressure_cv{megapascal},volume]
</properties>
    <trajectory filename='xc' stride='10'>x_centroid{angstrom}</trajectory>
    <trajectory filename='pos' stride='10'> positions </trajectory>
  </output>
  <total_steps> 400000 </total_steps>
  <prng>
    <seed>32345</seed>
  </prng>
  <ffsocket name='lmpserial' mode='unix'>
    <address>fixatoms</address>
  </ffsocket>
  <system>
    <initialize nbeads='4'>
      <file mode='pdb'> 3acn_e.pdb </file>
      <velocities mode='thermal' units='kelvin'> 200 </velocities>
    </initialize>
    <forces>
      <force forcefield='lmpserial'>  </force>
    </forces>
    <ensemble>
      <temperature units='kelvin'>200</temperature>
    </ensemble>
    <motion mode='dynamics'>
      <dynamics mode='nvt'>
        <thermostat mode='langevin'>
          <tau units='femtosecond'> 5 </tau>
        </thermostat>
        <timestep units='femtosecond'> 0.25 </timestep>
      </dynamics>
      <fixcom> False </fixcom>
      <fixatoms> [1, 2] </fixatoms>
    </motion>
  </system>
</simulation>
```